JOURNAL OF MATERIALS SCIENCE 28 (1993) 3137–3144

The reverse transformations in a high-strength high-hardenability Fe–C–Si–Mn–Mo steel

A. ALI
Metallurgy Division, Dr A. Q. Khan, Research Laboratories, PO Box 502, Rawalpindi, Pakistan

H. K. D. H. BHADESHIA
Department of Materials Science and Metallurgy, University of Cambridge, Cambridge, CB2 3QZ, UK

The kinetics of the reverse transformations from a mixture of bainitic ferrite and residual austenite to austenite have been investigated in a steel containing a relatively high silicon concentration. It was found that the reaustenitization process was initially rapid but slow at the end of reaction and the extent of austenite formed increased with increasing reaustenitization temperature until all of the bainitic ferrite had been transformed to austenite. The process of reaustenitization was followed by dilatometry, optical and transmission electron microscopy, and stereology. The results suggested that the formation of austenite took place by the movement of planar ferrite/austenite interfaces.

1. Introduction

The process of reaustenitization is an important phenomenon and is of considerable industrial importance. It plays an important role in several methods involving the heat treatment of steels, for example, the dual-phase steels which consist of a strong phase "martensite" as a load-carrying constituent in a ductile ferrite matrix. These steels are produced by intercritical annealing of low carbon alloy steels in the $\alpha + \gamma$ phase field to generate a mixture of ferrite and austenite, which is then quenched to induce martensitic transformation of the austenite. The martensitic regions may, in fact, contain some retained austenite and/or lower bainite as well, depending on the chemical composition and the cooling rate of the steel.

Austenite formation is also important in many fabrication processes involving multipass welding. In multilayer weld deposits, the heat input associated with the deposition of new layers, reheats the underlying microstructure to temperatures where austenite formation can occur [1]. The new austenite then cools and transforms back to a microstructure which can be rather different from that obtained immediately after weld deposition. Because many of the alloys used in the deposition of high-strength welds are designed to transform ultimately into bainitic microstructures, it is useful to study the reaustenitization process by heating such microstructures.

The formation of austenite from a variety of microstructures has previously been studied by Nehrenberg [2], Matsuda and Okamura [3, 4], Law and Edmonds [5], Yang [6], and Yang and Bhadeshia [7]. Recently, Yang and Bhadeshia [7] investigated the growth of austenite from bainite and acicular ferrite. They studied isothermal and continuous heating transformations. With isothermal transformation, they found that reverse transformation did not happen immediately when the temperature was raised above that at which the bainite or acicular ferrite had formed, even though the alloy was within the intercritical region of the phase diagram.

Most of the previous work was carried out on materials in which bainite forms together with other diffusional microstructures, e.g. pearlite, and led many researchers to incorrect interpretations. Furthermore, most of the work largely emphasized the nucleation and morphological studies. The present study deals with the reaustenitization process from a starting microstructure which is a mixture of bainite and residual austenite (the term residual austenite is used to represent the austenite which is left untransformed at the temperature where bainite is allowed to grow). Particular emphasis is placed on the mechanism and kinetics of the reaustenitization process in wrought steels.

2. Experimental procedure

2.1. Material selection

The steel selected for the present study is one which contains high silicon and manganese concentrations as the major alloying elements. The silicon retards the growth of cementite, so that a microstructure of just bainitic ferrite and residual austenite can be obtained by the transformation of austenite below the bainite-start, (B_s), temperature [8]. Such alloys are becoming more prominent in industry, both as wrought materials [9] and in the form of high silicon cast irons [10]. Manganese and molybdenum increase the incubation

0022–2461

TABLE I Chemical composition of the steel used in the present study

Element	Composition (wt %)
Carbon	0.22
Silicon	2.03
Manganese	3.00
Molybdenum	0.7
Titanium	0.004 ± 0.01
Aluminium	0.005 ± 0.02
Oxygen	94 p.p.m.
Iron	Balance

time for the formation of diffusional transformation products such as allotriomorphic ferrite, and generally raise the hardenability of the steel. The detailed chemical composition of the steel used in the present study is given in Table I.

2.2. Heat treatments

High-speed dilatometry was utilized to study the kinetics of reaustenitization. All the samples were homogenized at 1250 °C for 3 days prior to dilatometric experiments. All heat treatments were performed in a Theta industries high-speed dilatometer. The samples were first austenitized at 900 °C for 5 min, isothermally transformed at a temperature $T_b = 400$ °C for 2000 s to obtain a mixture of bainitic ferrite plus residual austenite and then, instead of cooling the specimens to ambient temperature, they were heated rapidly to an elevated temperature above T_γ for isothermal reaustenitization. A schematic diagram of the heat-treatment cycles is shown in Fig. 1.

2.3. Microscopy

Specimens for optical and transmission electron microscopy (TEM) were obtained from heat-treated samples and prepared as discussed elsewhere [11]. Thin-foil samples were examined using a Philips EM 400T transmission electron microscope, equipped with a Link EDX system to facilitate energy dispersive X-ray (EDX) analysis.

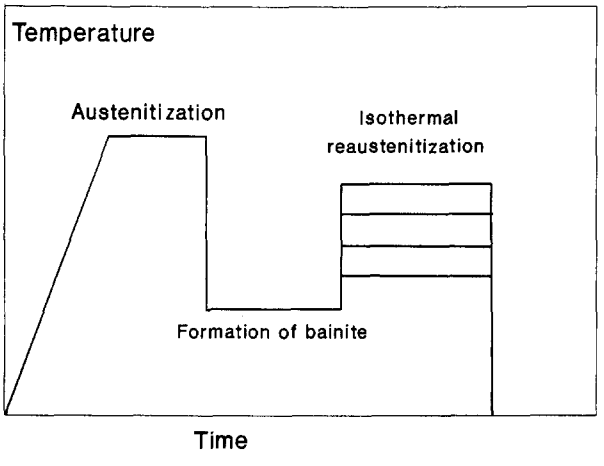

Figure 1 Schematic representation of the heat-treatment cycles used in the present study.

3. Results

The general microstructure is illustrated in Fig. 2 and, as expected, consisted of a mixture of bainitic ferrite, retained austenite and some martensite resulting from the decomposition of the residual austenite after cooling from the bainite formation temperature.

3.1. Dilatometry

The first detectable growth of austenite was found to occur at 660 °C as illustrated in Fig. 3; note that a length contraction is expected as ferrite transforms to austenite. In all cases, the transformation rate was initially rapid, but decreased with time at the isothermal reaustenitization temperature, T_γ, so that the specimen length eventually stopped changing. The maximum relative length change as a function of T_γ is plotted in Fig. 4. The results showed that $\Delta L/L$ increases as T_γ increases from 660 °C to 740 °C and then remains essentially constant with the further increase

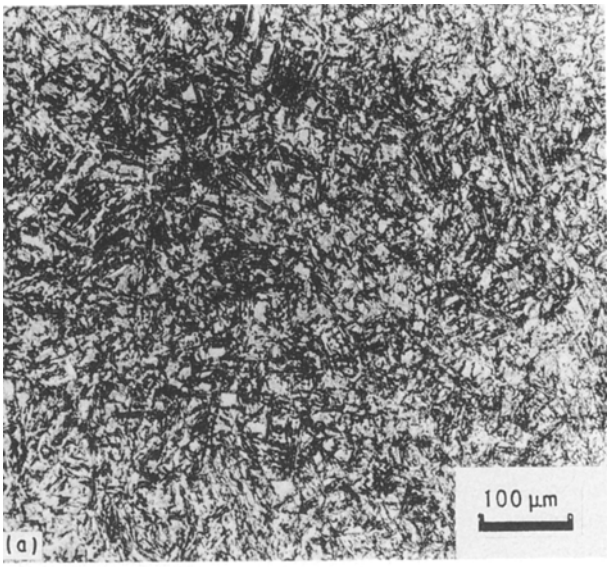

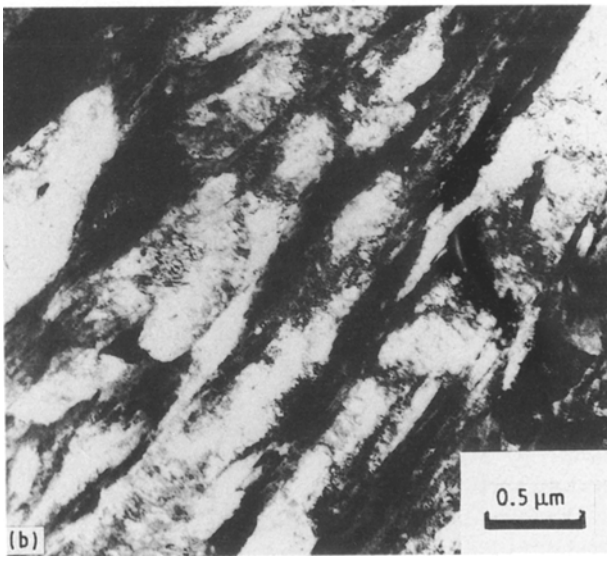

Figure 2 Typical mixed microstructure of bainitic ferrite, retained austenite and martensite after isothermal transformation at 400 °C for 2000 s followed by water quenching. (a) Optical micrograph (b) transmission electron micrograph.

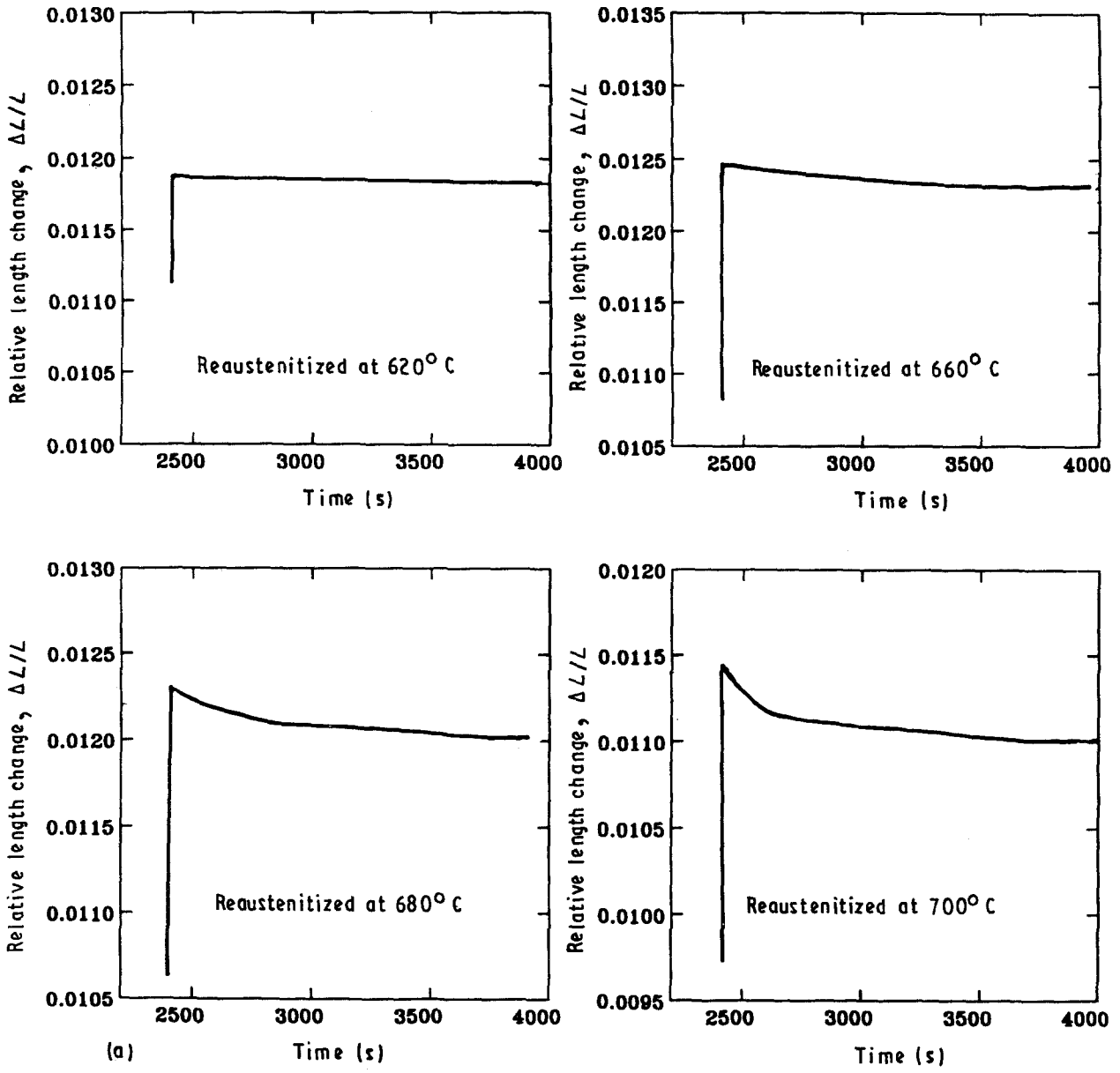

Figure 3 Isothermal reaustenitization studied using dilatometry. The specimens were initially isothermally transformed to bainite at 400 °C for 2000 s and then rapidly heated to the isothermal reaustenitization temperature indicated on each figure.

in T_γ to 860 °C. The maximum degree of transformation to austenite thus increases from nearly zero at 620 °C to complete reverse transformation at above 740 °C. It is also seen from the Fig. 4, that the rate of ferrite to austenite transformation increases with T_γ.

3.2. Transmission electron microscopy

The phenomenon of reaustenitization can be monitored by observing the thickening of austenite layers using transmission electron microscopy (Fig. 5). The bainitic microstructure observed at 400 °C is shown in Fig. 5a. Fig. 5b is a micrograph from specimen reaustenitized at 660 °C, in which the ferrite subunits are parallel to each other and are separated by the austenite layers (now become martensite after cooling to ambient temperature). The thickness of the austenite films does not seem to increase significantly at 660 °C as expected from the dilatometric results (Fig. 3). As the isothermal reaustenitization temperature increases, the austenite films become detectably thicker (Fig. 5c–d). However, the austenite layers still retain their general form as shown in Fig. 5e for reaustenitization at 740 °C. Fig. 5f shows that there is some ferrite retained even after reaustenitization at 780 °C. The electron micrographs in Fig. 5g demonstrates completely martensitic structure, indicating the completion of austenitization following the 860 °C heat treatment. This also confirms the dilatometric data (Fig. 4), that the maximum length change achieved beyond about 780 °C does not vary much with T_γ. A slight decrease is, in fact, expected as T_γ rises, even though the samples fully reaustenitized, because the difference in austenite and ferrite densities decreases with rising temperature.

3.3. Microanalysis

The microanalysis results are given in Table II and shown in Fig. 6 for a range of isothermal reaustenitization temperatures. Fig. 6 shows that the degree of

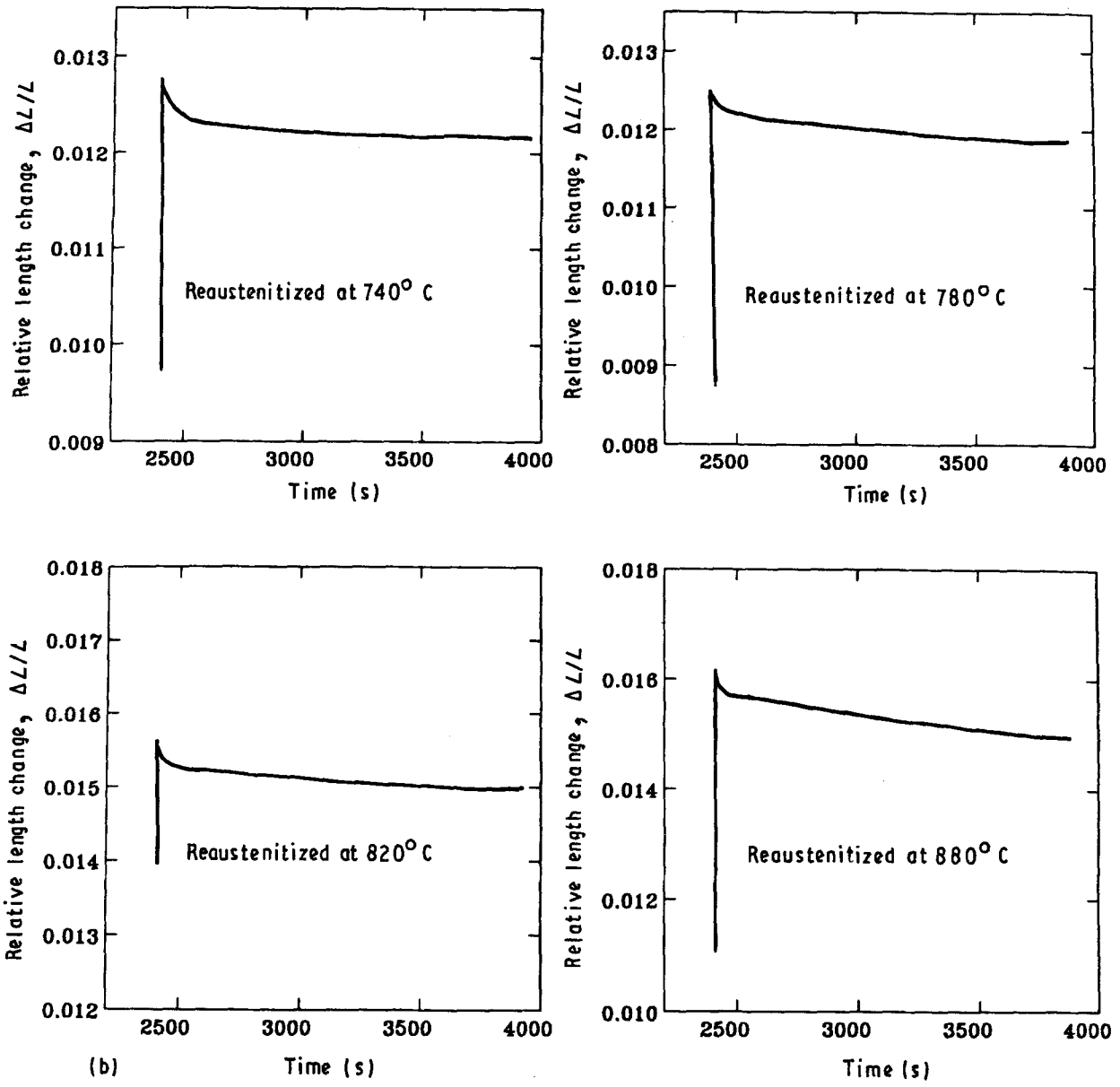

Figure 3 (continued)

partitioning of substitutional alloying elements increases with increasing austenitization temperature.

3.4. Hardness

The hardness of each specimen was measured after the isothermal reaustenitization and the results are plotted in Fig. 7. The results show that the hardness achieves a maximum value after austenitization at about 780 °C.

TABLE II EDX analysis of the matrix and ferrite. All the specimens were austenitized at 900 °C for 5 min and then transformed to bainite at 400 °C for 2000 s prior to reaustenitization.

	Temperature (°C)	EDX analysis (wt %)			
		Fe	Mn	Si	Mo
Matrix	620	93.7 ± 1.2	3.4 ± 0.7	2.1 ± 0.2	0.6 ± 0.3
	660	93.6 ± 0.7	3.3 ± 0.5	2.1 ± 0.4	0.9 ± 0.5
	680	94.2 ± 0.7	3.3 ± 0.4	1.9 ± 0.4	0.6 ± 0.3
	700	94.1 ± 0.7	3.4 ± 0.6	1.9 ± 0.4	0.6 ± 0.5
	860	94.1 ± 0.6	3.2 ± 0.3	1.9 ± 0.1	0.7 ± 0.4
Ferrite	620	94.1 ± 0.7	2.7 ± 0.5	2.3 ± 0.3	0.9 ± 0.7
	660	95.0 ± 0.9	2.4 ± 0.4	2.0 ± 0.4	0.5 ± 0.6
	680	95.1 ± 0.9	2.3 ± 0.4	1.9 ± 0.4	0.6 ± 0.3
	700	94.6 ± 0.7	2.5 ± 0.8	2.1 ± 0.5	0.7 ± 0.5
	860	94.5 ± 0.7	2.4 ± 0.3	2.1 ± 0.2	0.9 ± 0.7

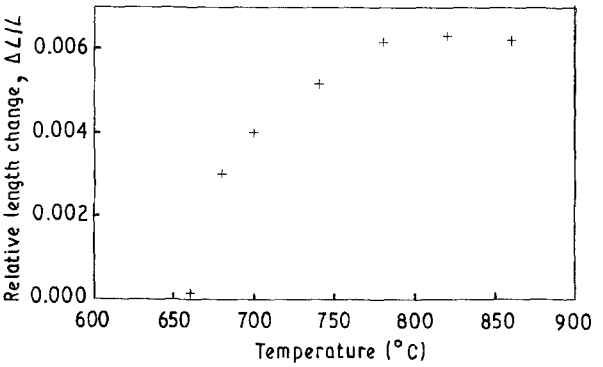

Figure 4 The maximum magnitude of the relative length change ($\Delta L/L$) increases with the reaustenitization temperature, T_γ, and then attains an approximately constant value after the sample achieved a fully austenitic state. Note that all the length changes are, in fact, negative.

4. Discussion

The results obtained in this study generally support the conclusions published earlier [6, 7] drawn from experiments on reaustenitization from weld deposits and provide additional microstructural detail. The Yang and Bhadeshia model [7] shows that because isothermal transformation of austenite to bainite ceases prematurely before the austenite achieves its

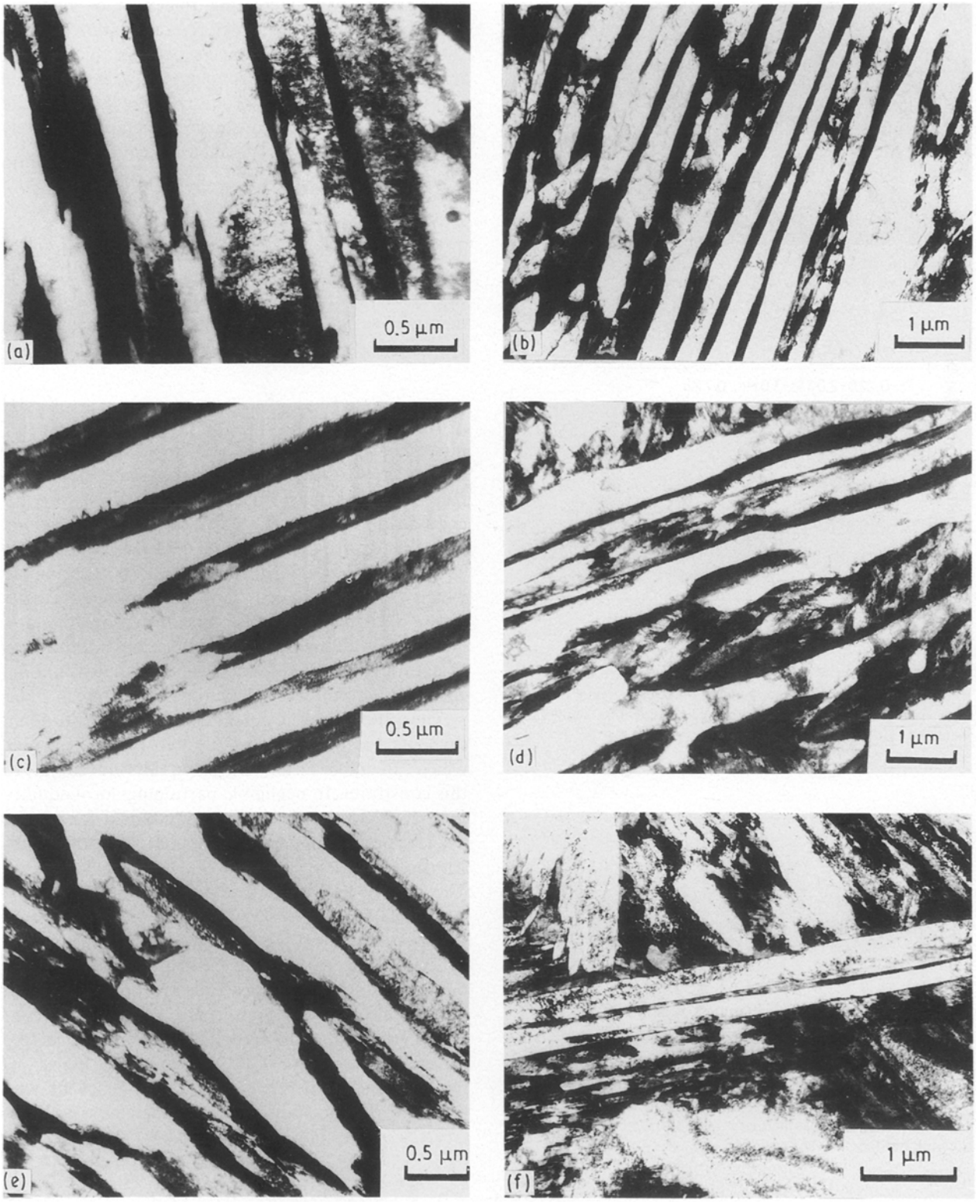

Figure 5 Transmission electron micrographs showing the reaustenitization from bainitic microstructure. (a) Transformed bainitic microstructure, $T_b = 400\,°C$; (b) microstructure of the specimen isothermally reaustenitized at 620 °C for 2000 s; note that there is some rounding of the bainite sub-units at their tips, $T_\gamma = 660\,°C$. (c, d) Transmission electron micrographs showing the thickening of the residual austenite films after isothermal reaustenitization for 3000 s at (c) $T_\gamma = 680\,°C$, (d) $T_\gamma = 700\,°C$; note that the films remain parallel to the ferrite sub-units; (e) $T_\gamma = 740\,°C$. (f) Although most of the microstructure reaustenitized, some of the ferrite subunits are still present after isothermal reaustenitization at 780 °C for 3000 s, $T_\gamma = 780\,°C$. (g) The specimen completely reaustenitized after isothermal transformation for 3000 s at 860 °C, $T_\gamma = 860\,°C$.

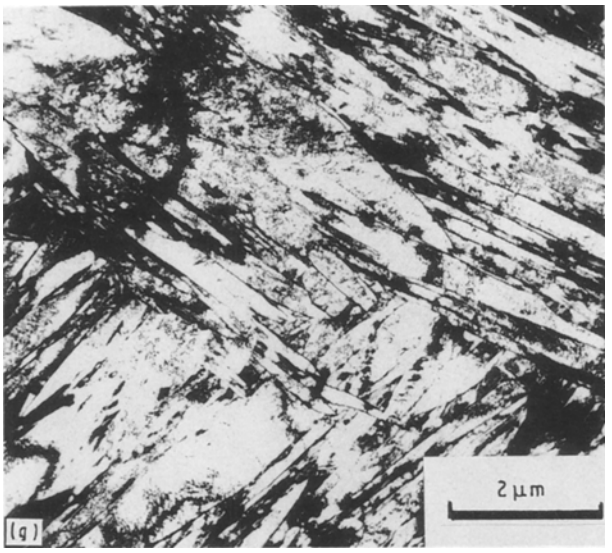

Figure 5 (continued)

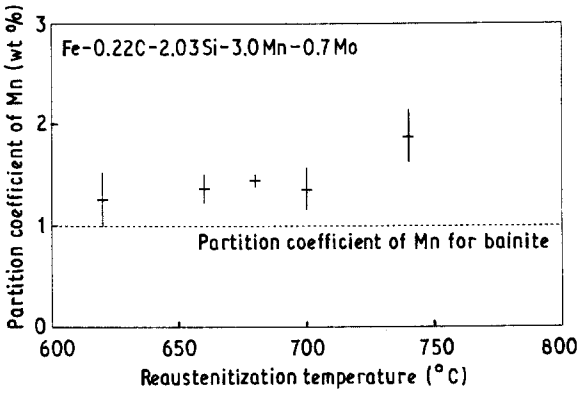

Figure 6 The effect of reaustenitization temperature on the partition coefficient of manganese, showing that the degree of partitioning of manganese increases as the reaustenitization temperature increases.

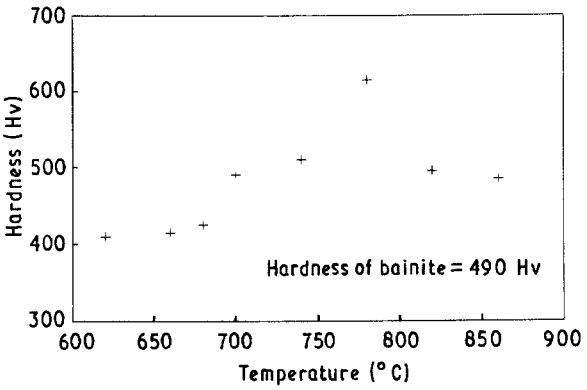

Figure 7 The effect of isothermal reaustenitization temperature on the bulk hardness of the specimens.

equilibrium carbon concentration, there is a large temperature hysteresis before the reverse transformation to austenite becomes possible during heating from the bainite transformation temperatures. No reverse transformation to austenite can occur until the sample is heated to an elevated temperature where the residual austenite composition becomes identical to the composition given by the Ae'_3 phase boundary. This leads to a large hysteresis in the forward and reverse transformation temperatures for austenite, a hysteresis which is not found when the starting microstructure is a mixture of allotriomorphic ferrite and austenite. This is evident from transmission electron micrographs with increasing thickness of austenite layers as shown in Fig. 5. A close examination of Fig. 5 shows that as austenite layers become thicker they retain their layer-like morphology between the ferrite sub-units. This provides strong evidence that austenite grows by the normal movement of the approximately planar α/γ interface as assumed by Yang [6].

4.1. EDX analysis

The results of energy dispersive X-ray analysis of isothermally reaustenitized specimens show that the degree of partitioning of substitutional alloying elements, x_i, as indicated by the deviation of the partition coefficient, K_i, from unity, where

$$K_i = \frac{x_i^\gamma}{x_i^\alpha} \quad (1)$$

increases with increasing reaustenitization temperature (Fig. 6). As the driving force for reaustenitization increases, the transformation tends towards para-equilibrium or negligible partition–local equilibrium; this is illustrated clearly by the data for 700 °C. Para-equilibrium is a state of constrained equilibrium in which the substitutional lattice is configurationally frozen with respect to the transformation interface. Hence, even though the transformation is diffusional in nature, the ratio (atomic fraction of substitutional element (i)/atomic fraction of iron) is the same in α and γ. Thus, the chemical potentials of the substitutional elements are not equal in the two phases. Carbon, which can diffuse faster, reaches equilibrium subject to this constraint. In negligible partioning–local equilibrium (NPLE), equilibrium is maintained for all the transformation interface, but the concentration of substitutional element is essentially the same in all phases. The results also show that as the thickness of the austenite layers increases with time for a given T_γ, the partition coefficient, K_i, changes, indicating that the concentrations of alloying elements at the interface during the growth of austenite are not equilibrium concentrations. These results are qualitatively consistent with the dilatometric data. One of the factors for the increased rate of transformation at high T_γ is the fact that the degree of redistribution of alloying elements during transformation increases with increasing T_γ.

4.2. Carbon concentration of the residual austenite

The carbon content of the residual austenite when isothermal transformation ceases is very useful in understanding the transformation mechanism. Because of the relatively high silicon concentration in the steel used, the precipitation of cementite tends to be

rather sluggish. Consequently, isothermal transformation to upper bainite generates a microstructure consisting of carbide-free bainitic ferrite and carbon-enriched residual austenite. It is then possible to estimate the carbon concentration, x_γ, of the residual austenite using a simple mass balance procedure, if the volume fraction of bainitic ferrite, V_b, is known

$$x_\gamma = \frac{\bar{x} - (V_b x_\alpha)}{1 - V_b} \quad (2)$$

where $\bar{x}$ is the average carbon concentration of the alloy and x_α is the carbon concentration of the bainitic ferrite. The volume fraction, V_b, can be calculated from the dilatometric data as discussed by Bhadeshia [1]. The values of x_γ estimated by using the procedures just described here, for the point where isothermal transformation ceases at any given temperature, are plotted on the phase diagram presented in Fig. 8. The phase boundaries were calculated using the method given by Bhadeshia and Edmonds [9]. The data presented in Fig. 8 confirm that the formation of upper bainite stops prematurely, well before the carbon concentration of the residual austenite reaches the para-equilibrium Ae'_3 phase boundary. This effect is known as the incomplete reaction phenomenon [9]. After isothermal transformation to bainite at the temperature T_b has ceased, if the sample is rapidly heated to an isothermal temperature, T_γ, for reaustenitization, the reverse transformation to austenite does not require any nucleation, but simply the movements of already existing ferrite–austenite interfaces, because the bainitic ferrite consist of ferrite sub-units which are approximately parallel to each other. The thickness of austenite films measured by stereology is given in Fig. 9, which shows that as the reaustenitization temperature increases the austenite films between bainitic ferrite become thicker and eventually consumes all the bainitic ferrite transformed to austenite, i.e. above 780 °C. This is also confirmed by the transmission electron microscopy.

4.3. Macrohardness

The hardness of the reaustenitized samples after quenching to ambient temperature has been found to

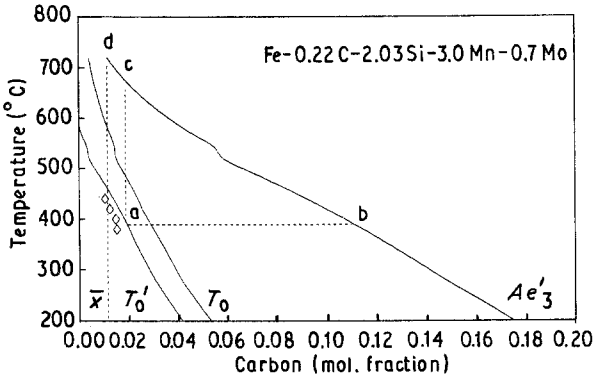

Figure 8 Calculated phase diagram with experimental data of carbon concentration of residual austenite at the termination of isothermal transformation. The para-equilibrium phase boundaries Ae'_3, T_0 and T'_0 were calculated as in [9].

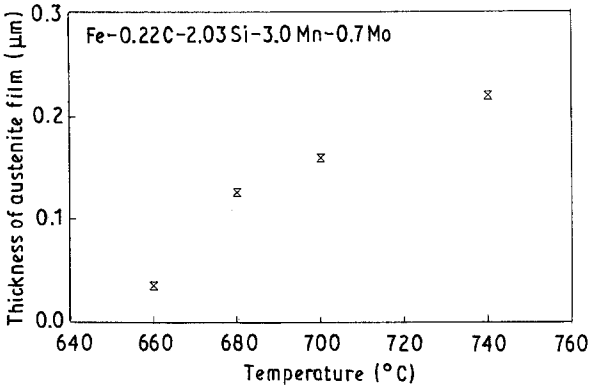

Figure 9 Measurement of the thickness of the residual austenite films. The thickness of the austenite films increases with increasing reaustenitization temperature.

increase initially as with the isothermal reaustenitization temperature. This increase is expected because the amount of austenite (and hence martensite) at the austenitization temperature increases with T_γ. The maximum value of about 600 Hv observed at around 780 °C beyond which the sample becomes fully austenitic, is more difficult to understand, but could arise because samples quenched from higher temperatures undergo a greater degree of autotempering of the martensite.

5. Theory for reaustenitization

In this section the thermodynamic model presented by Yang and Bhadeshia [7] for the interpretation of the observations on reaustenitization from a starting microstructure of bainite and retained austenite are analysed in the light of the results obtained in the present study. Because after the diffusionless growth of bainite, carbon is rapidly and spontaneously redistributed into the residual austenite with an accompanying reduction in free energy, the α_b/γ transformation in its original form is irreversible. The problem of reaustenitization is therefore considerably different from the case of martensite to austenite in, for example, shape-memory alloys. It is noted that the formation of bainite ceases prematurely during isothermal transformation when the carbon content of the residual austenite reaches the T'_0 curve (the phase diagram for the alloy is presented in Fig. 8). It follows that the carbon concentration, x_γ, of the residual austenite when the formation of bainite cease at T_b, is given by (point marked "a" in Fig. 8).

$$x_\gamma = x_{T'_0} \quad (3)$$

furthermore, it is noted that

$$x_\gamma \ll x_{Ae'_3} \quad (4)$$

where $x_{Ae'_3}$ is marked "b" in Fig. 8. Thus, although the formation of bainite ceases at T_b, because $x_\gamma \ll x_{Ae'_3}$, the driving force for austenite to transform diffusionally to ferrite is still negative. Another way of expressing this is to say that the volume fraction of bainite present when its formation ceases at T_b is much less than is required by the Lever rule. In fact, this remains the case until the temperature, T, is high

enough, i.e. $T = T_\gamma$, to satisfy the equation

$$x_\gamma = x_{Ae'_3} \quad (5)$$

Hence, reaustenitization will first occur at a temperature T_γ, as indicated in Fig. 8 (marked c), and as observed experimentally. Note that this is a direct consequence of the mechanism of the bainite transformation, which does not allow the transformation to reach completion. The theory goes further than explaining just the temperature at which the reverse transformation should begin. It also predicts that at any temperature, T, greater than T_γ, the reverse $\alpha \rightarrow \gamma$ transformation should cease as soon as the residual austenite carbon concentration x'_γ (initially x_γ) reaches the Ae'_3 curve, i.e. when

$$x'_\gamma = x_{Ae'_3} \quad (6)$$

with the equilibrium volume fraction of austenite at the temperature T_γ, the volume fraction of austenite, V_γ, being given by the expression

$$V_\gamma = \frac{\bar{x}}{x_{Ae'_3}} \quad (7)$$

Assuming that the carbon concentration of ferrite is negligible and $x_{Ae'_3} > \bar{x}$ when $x_{Ae'_3} = \bar{x}$, the alloy eventually becomes fully austenitic (point "d" in Fig. 8), and if this condition is satisfied at $T = T_\gamma$, then at all $T > T_\gamma$, the alloy transforms completely to austenite. These concepts immediately explain the dilatometric data in which the degree of $\alpha \rightarrow \gamma$ transformation increase (from zero at 660 °C) with the temperature of isothermal reaustenitization, until the temperature 780 °C, where the alloy transforms completely to austenite.

6. Conclusions

The kinetics of reaustenitization in relatively high silicon concentrations has been studied by a combination of techniques such as high-speed dilatometry, transmission electron microscopy, EDX analysis, stereology and macrohardness. It is found that the formation of austenite increases with increasing reaustenitization temperatures and at 780 °C all the bainitic ferrite transformed to austenite. The transformation is initially rapid but slow at the end of reaction. The formation of austenite was found to take place by the movements of planar ferrite/austenite interfaces. It is confirmed by measuring the thickness of the austenite films which increase during the reaustenitization process.

Acknowledgements

The authors are grateful to Professor C. J. Humphreys for the provision of laboratory facilities at the University of Cambridge, and Dr A. Q. Khan, Research Laboratories of Pakistan, for financial support.

References

1. H. K. D. H. BHADESHIA, *Metal Sci.* **16** (1982) 159.
2. A. E. NEHRENBERG, *Trans. Met. Soc. AIME* **188** (1950) 162.
3. S. MATSUDA and Y. OKAMURA, *Trans. ISIJ.* **14** (1974) 363.
4. *Idem, ibid.* **14** (1974) 444.
5. N. C. LAW and D. V. EDMONDS, *Metall. Trans.* **11A** (1980) 33.
6. J-R. YANG, PhD thesis, University of Cambridge, UK (1987).
7. J-R. YANG and H. K. D. H. BHADESHIA, *Mater. Sci. Engng* **A118** (1989) 155.
8. R. F. HEHEMANN, in "Proceedings of the Phase Transformations", (ASM, Metals Park, OH, 1970) pp. 307.
9. H. K. D. H. BHADESHIA and D. V. EDMONDS, *Metall. Trans.* **10A** (1979) 895.
10. K. B. RUNDMAN, D. J. MOORE, K. L. HAYRYNEN, W. J. DUBENSKY and T. N. ROUNS, *J. Heat Treating* **5** (1988) 79.
11. A. ALI, PhD thesis, University of Cambridge, UK (1991).

Received 2 September
and accepted 30 October 1992